Princeton Plasma Physics Laboratory

PPPL- 4563

PPPL- 4563

He Puff System For Dust Detector Upgrade

B. Rais, C.H. Skinner A.L. Roquemore

September, 2010

Prepared for the U.S. Department of Energy under Contract DE-AC02-09CH11466.

Princeton Plasma Physics Laboratory
Report Disclaimers

Full Legal Disclaimer

Trademark Disclaimer

PPPL Report Availability

Princeton Plasma Physics Laboratory:

http://www.pppl.gov/techreports.cfm

Office of Scientific and Technical Information (OSTI):

http://www.osti.gov/bridge

Related Links:

U.S. Department of Energy

Office of Scientific and Technical Information

Fusion Links

Submitted for PPPL report 28 September, 2010

He puff system for dust detector upgrade.

B. Rais[1], C.H. Skinner[2] A.L. Roquemore[2]

[1]*Université de Provence, Aix-Marseille, PACA, 13001, France*

[2]*Princeton Plasma Physics Laboratory, Princeton, N. J., 08543, USA*

Abstract

Local detection of surface dust is needed for the safe operation of next-step magnetic fusion devices such as ITER. An electrostatic dust detector, based on a 5 cm x 5 cm grid of interlocking circuit traces biased to 50 V, has been developed to detect dust on remote surfaces and was successfully tested for the first time on the National Spherical Torus Experiment (NSTX). We report on a helium puff system that clears residual dust from this detector and any incident debris or fibers that might cause a permanent short circuit. The entire surface of the detector was cleared of carbon particles by two consecutive helium puffs delivered by three nozzles of 0.45 mm inside diameter. The optimal configuration was found to be with the nozzles at an angle of 30º with respect to the surface of the detector and a helium backing pressure of 6 bar.

1. Introduction

Dust production in next-step magnetic fusion devices will be significantly higher than in contemporary devices due to the more intense plasma wall interactions and the increase in erosion levels[1]. Local measurements of surface dust are part of the ITER dust strategy [2] and an absolute detection accuracy of 50% has been specified [3].

A novel device to detect the settling of dust particles on remote surfaces has recently been demonstrated on NSTX [4]. A grid of two closely interlocking conductive traces on a circuit board was biased to 50 V (Fig. 1). Dust particles that fall on the detector cause a transient short circuit and create a voltage pulse that is recorded by standard nuclear counting electronics. Large debris (> 90 μm) and fibers that might cause a permanent short circuit are prevented from reaching the detector by a cover mesh. The total number of counts is proportional to the mass of dust impinging on the detector [5]. Typically 90% of the total number of particles that land on the detector are vaporized by the current pulse and ejected from the detector, however about 10% may remain on the surface of the detector [6]. These may produce signals at a later time, complicating efforts to correlate the dust signal with plasma events. Initial work on a helium puff system to clear residual dust from the detector is described in ref [7]. The system consisted of a volume pressurized with helium gas, a piezoelectric valve and a nozzle aimed at the surface of the detector at a 45º angle. The gas puff system was able to clear a 4 cm x 4 cm area of carbon particles and 3 cm x 3 cm with tungsten particles but limitations in the throughput of the piezoelectric valve controlling the gas flow prevented coverage of the entire 5 cm x 5 cm surface of the detector.

We report on the development of a new system based on high throughput pneumatic valves that feed a manifold of small nozzles aimed on the surface of the detector and mesh. We note that such a puffer system may also be useful for an alternative dust detection technique based on a capacitive diaphragm manometer that measures the accumulated mass of dust [8]. Rezeroing such a detector by removing dust with a helium puff could address concerns with long term drifts.

2. Puffer optimal configuration and design

Our objective was to completely clear the surface of the detector of residual dust, with a minimal helium puff that could be easily handled by the tokamak pumping system. High throughput pneumatic valves were used to increase the gas flow rate from several nozzles that were aimed to cover the whole surface of the detector. The nozzles were designed to fit in the restricted space between the detector and the NSTX torus interface gate valve. In NSTX the dust detector was protected from larger debris and fibers with a cover mesh of 60% optical transmission and some particles were left on the wires of the mesh [5]. To clear these particles a fourth nozzle was aimed at the surface of the mesh. The system configuration was first optimized by imaging the cleared areas with a digital camera. Then the cleaning efficiency was measured with the dust detector itself.

2.1. Single nozzle setup

The schematic of the experimental setup is shown in Fig. 2. The system consists of a helium tank, a regulator, a shut-off valve, a pressure gauge, and two pneumatic valves that confine a pressurized plenum. The pneumatic valves have an i.d. of 3.8 mm and a flow coefficient Kv of 0.26 m^3/h and are compatible with the magnetic environment of a tokamak. The total volume of the plenum (including the internal volume of the valves) was measured by filling the volume with ethanol from a burette and was 5.2 cm^3. The plenum was then connected to the exit nozzle(s) by a short 1 cm^3 volume tube to maximize the gas puff pressure at the detector. To deliver a helium puff the helium tank valve was opened and the plenum was pressurized to 6 bar by opening the pneumatic valve 1 in Fig. 2. The tank shut off valve and pneumatic valve 1 were then closed. The helium puff was released by opening pneumatic valve 2. The total expelled helium per puff was 32.4 $bar \cdot cm^3$ when the puff system operated at a pressure of 6 bar.

First experiments were performed with the gas puff system connected to a single nozzle to investigate the dust clearing efficiency as a function of plenum pressure, nozzle incidence angle and distance from detector. Tests were performed with sand particles spread evenly over the surface of a 6 cm x 6 cm Garolite G-10/FR4 piece, at atmospheric pressure. A 5 cm x 5 cm area

was marked to indicate the area of the 51 mm electrostatic dust detector. The sand particles were easily visible once spread on the G-10 piece. A schematic of the setup and the nozzle configuration is shown in Fig. 3. The area cleared by the helium puff was measured by comparing images taken by a digital camera before and after puffing. These first experiments provided useful information regarding the properties and functioning of the system. It was observed that the cleared area was greater if the nozzle was positioned on the very edge of the 5 cm x 5 cm surface of the G-10 piece at a height of 1 mm.

To determine the most effective backing pressure helium was puffed on to sand particles at pressures of 2 bar, 3.5 bar, 5 bar and 6 bar at an angle of incidence of 30º. The results are presented in Fig. 4 and show that the highest % cleared area was obtained at 6 bar. The same setup was used to obtain the optimal nozzle inclination; incidence angles of 30º, 45º, 60º and 90º were used for backing pressures of 5 and 6 bar and the effect recorded with the digital camera. The results are shown in Fig. 5.

The optimal configuration that demonstrates maximum clearance of the surface of the detector was found to be a plenum pressure of 6 bar, an incidence angle of 30º and the nozzle at the edge of the surface to be cleared at a height of 1 mm. Fig. 6 shows pictures taken with the camera before and after puffing sand particles. It can be seen that 80% of the area was cleared with the optimal configuration; however some sand was left at the corners.

2.2. Multiple nozzle puffer

In order to attain complete clearance of the surface, two additional nozzles were added to the previous setup. These are parallel to and 13 mm either side of the first nozzle. In the perpendicular plane all nozzles had the most efficient incidence angle of 30° and a height of 1 mm above the detector as optimized previously.

The three-nozzle manifold was designed to fit on a 15 cm conflat flange and operate with an incidence angle of 30º to the surface of the 51 mm square dust detector as shown in Fig. 7. The puff system was set up in a vacuum chamber and first tested at atmospheric pressure and then in vacuum (section 3) to simulate the environment in NSTX. Sand particles or carbon powder

scraped from ATJ tile were spread on top of the 6 cm x 6 cm Garolite G-10/FR4 piece, which in turn was mounted on a 15 cm flange attached to the chamber. Fig. 8 shows images taken with a digital camera, that viewed the particles through a window on the upper side of the chamber. It was observed that after one puff the entire surface of the G-10 piece was cleared, however some sand particles landed back on the surface after bouncing off the vacuum chamber. After a second puff the area was totally cleared. Fig. 9 shows results with carbon powder. In this case the entire 5 cm x 5 cm surface was free of visible dust after one puff.

3. Vacuum puffing with the 51 mm detector

The electrostatic dust detector can detect particles of μm scale that are not resolved in the photographic images. The dust detector was operated in vacuum to further test the efficacy of the helium puff system. Carbon particles, scraped from ATJ tiles were dried by baking them in an oven for four hours at 100 °C, to minimize moisture effects and simulate dust in the NSTX vacuum chamber.

The helium puffer was set up along with the dust detector on the 15 cm flange in the vacuum chamber as shown in Fig. 10. The detector was connected to the detection electronics described in refs. [4,5]. To limit the potential over-pressure hazard in case of failure of the pneumatic valves or the mechanical pump a pressure relief valve was mounted on the chamber that automatically vented pressures in excess of 0.5 bar above atmospheric. In addition, lexane shields covered the viewports.

The dust was delivered by a tray with a mesh bottom mounted on the upper flange as described in ref. [9]. The chamber was evacuated by a mechanical pump to a pressure below 5 mTorr. Carbon dust was delivered to the energized detector by knocking on the upper flange of the chamber until a predetermined number of counts was reached on the detector electronics [5]. The chamber was then slowly vented and the dust tray was removed to prevent further dust falling on the detector. Once the chamber was again sealed and evacuated without the dust tray, helium puffs were used to clear residual dust from the surface of the detector.

Any residual dust that remains on the detector can be disturbed by the helium puff or a mechanical knock. Dust that produces breakdown between the energized traces will produce a current pulse and be detected. The basic procedure to test the efficiency of the puff system was to perform a sequence of helium puffs and mechanical knocks and observe any increase in the number of counts. This was repeated until no additional counts were triggered after several knocks indicating that the entire surface of the detector was cleared of dust.

Fig. 11 shows the percentage of additional counts that occurred after successive puff-knock events. It can be seen that the first puff could trigger about 3% of additional counts followed by about 1% due to a knock on the chamber. Subsequent puffs after the first two, caused less than 0.5% of additional counts indicating that two puffs were sufficient to almost entirely clear the surface of the 51 mm detector of residual dust.

After testing the efficiency of the puff system on the 51 mm detector, a cover mesh was added above the detector to mimic the setup used in NSTX [4]. A fourth nozzle was added to clear dust from the mesh and the system tested with carbon dust. The cover mesh was 18 mm above the detector. This nozzle was 1 mm above the mesh with a 30 degrees incidence angle just as the three-nozzle configuration described previously. The mesh was supported by two walls parallel to the direction of the flow of helium with four louvres on each wall to facilitate flow of dust particles away from the detector and prevent them from bouncing back on the detector. This embodiment is shown in Fig. 12.

Fig. 13 shows the percentage of additional counts that occurred after successive puff-knock events in the case of the four nozzles manifold and the cover mesh above the 51 mm detector. Tests were done in vacuum. It was observed that after one initial helium puff up to 6% of extra counts were triggered by the first knock event. After a second puff, this number fell to less than 1% even after applying three successive knocks on the lower port of the chamber. This indicates that a significant amount of dust was held up on the wires of the cover mesh and fell on the detector after the first knock event. This is consistent with previous results [5] that showed a small decrease in the sensitivity of the detector due to dust holdup on cover mesh.

It can be seen that around 8.7% and 10.8% of total additional counts for the tests in vacuum without and with the cover mesh respectively, were triggered by 2 consecutive puff-knock events. The amount of additional counts dropped to less than 1% and no counts were triggered by puff/knock events after the fifth puff. These percentages are calculated from the counts generated by the puff/knock events divided by the initial counts recorded from the dust falling on the detector. The additional counts represent the amount of dust that did not promptly vaporize from the surface of the detector or was held on the wires of the cover mesh and was cleared by the puff system. These results are consistent with results from ref. [6] which reported that about 90% of the incident dust was vaporized and 10% remained on the surface of the detector. The present experiment showed that after two consecutive helium puffs less than 0.05% of residual dust was left on the surface of the detector.

4. Conclusion

In summary, we report on the development of a helium puff system designed to clear residual dust from the electrostatic dust detector. The configuration that demonstrated optimal clearance of the surface of the detector was found to have a 30º incidence angle and a plenum pressure of 6 bar. Such a puff system with one nozzle cleared sand particles from 80% of a 5 cm x 5 cm area however some particles were left at the corners. A three-nozzle manifold was then implemented to increase the area cleared but after one puff some particles were observed to land back on the surface after bouncing off the walls of the chamber. Two puffs successfully cleared the entire 25 cm^2 area. This result was confirmed by operating the puff system with carbon particles, the dust detector and detection electronics. A cover mesh, as used in NSTX, was added to the system and cleared of residual dust by a fourth nozzle. Results using the dust detection electronics confirmed that two consecutive He puffs were sufficient to completely clear the detector of more than 99.9 % of residual dust.

Acknowledgements

The authors would like to thank A. Opdenaker, M. Ono and T. Egebo for enabling this MSc thesis project to be performed in the US, and T. Holoman, D. Labrie, T. Provost, G. Smalley for invaluable technical assistance.

This work was funded by US DOE Grant No DE AC02-09CH11466.

Figure Captions

Fig. 1: Schematic of dust detector (not to scale) showing interlocking combs of traces. Dust impinging on the traces causes a short circuit and a voltage signal is generated across the 51 Ohm resistor.

Fig. 2: Schematic of the gas puff system (not to scale).

Fig. 3: Schematic of the setup used for tests to obtain the optimum plenum pressure and inclination angle of the puff system. The 6 cm x 6 cm area consists of the entire surface of the G-10 piece and the 5 cm x 5 cm area consists in the surface of the 51 mm detector to be cleared from residual dust.

Fig. 4: Percentage of the cleared area vs. the backing He pressure with an incidence angle of 30º. One nozzle was aimed with 1 mm height from the detector. The experiment was conducted in air at atmospheric pressure.

Fig. 5: The cleared area vs. the angle of incidence of the nozzle for 5 and 6 bar backing pressure. 1 mm distance separated the nozzle and the 5 cm x 5 cm area (surface of the electrostatic dust detector) and the experiment was conducted in air at atmospheric pressure. The cleared area % is defined as the area free of sand divided by the 5 cm x 5 cm area of the dust detector.

Fig. 6: Pictures of sand particles at atmospheric pressure taken with a digital camera before puff (a) and (c) and after puff (b) and (d) with one nozzle at 30º incidence angle. In image (b) the puff was performed with a plenum pressure of 5 bar and in image (d) with 6 bar. The puff was in the direction from left to right.

Fig. 7: Configuration of the three-nozzle puffer. The nozzles are aimed with a 30º incidence angle at 1mm above the 5 cm x 5 cm area (surface of the electrostatic dust detector). Sand particles were spread evenly of the 5 cm x 5 cm surface of the G-10 piece.

Fig. 8: Pictures of sand particles at atmospheric pressure taken with a digital camera before and after successive puffs. Puffing was achieved with the three-nozzle manifold with a 30º incidence angle and 6 bar plenum pressure. The three-nozzle manifold is localized on the left of the images and the puffs were achieved from left to right. The image has been color enhanced to make the sand particles more visible.

Fig. 9: Pictures of carbon particles in air at atmospheric pressure taken with digital camera (a) before puff and (b) after puff. Puffing was performed with the three-nozzle manifold with a 30º incidence angle and 6 bar plenum pressure. The images did not undergo any color enhancement.

Fig. 10: Setup used for vacuum puffing.

Fig. 11: Percentage of additional counts triggered by consecutive puffs labeled 1P, 2P, 3P … and knocks labeled 1K, 2K, 3K … in vacuum conditions without cover mesh and with the 3 nozzles

manifold. For three trials the percentage of additional counts triggered by a knock event after a second puff was lower than 0.5%.

Fig. 12: Puff system setup with 51mm dust detector and cover mesh used in NSTX [4,5]. The detector is shown schematically by the thick lines under the cover mesh. For clarity the mesh porosity is not to scale. Three of the nozzles are aimed on the surface of the detector and the fourth nozzle is aimed at the surface of the mesh.

Fig. 13: Percentage of additional counts triggered by consecutive puffs labeled 1P, 2P, 3P … and knocks labeled 1K, 2K, 3K … in vacuum conditions with cover mesh and 4 nozzles manifold. After two puffs an insignificant number of additional counts were triggered by a knock event indicating that the entire surface of the detector was cleared.

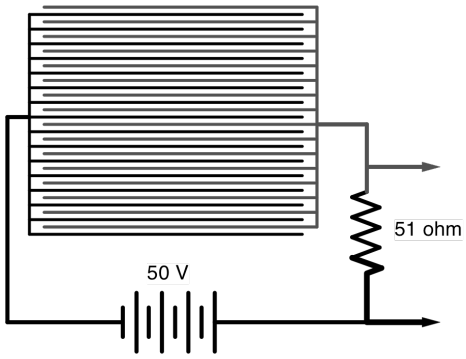

Fig. 1: Schematic of dust detector (not to scale) showing interlocking combs of traces. Dust impinging on the traces causes a short circuit and a voltage signal is generated across the 51 Ohm resistor.

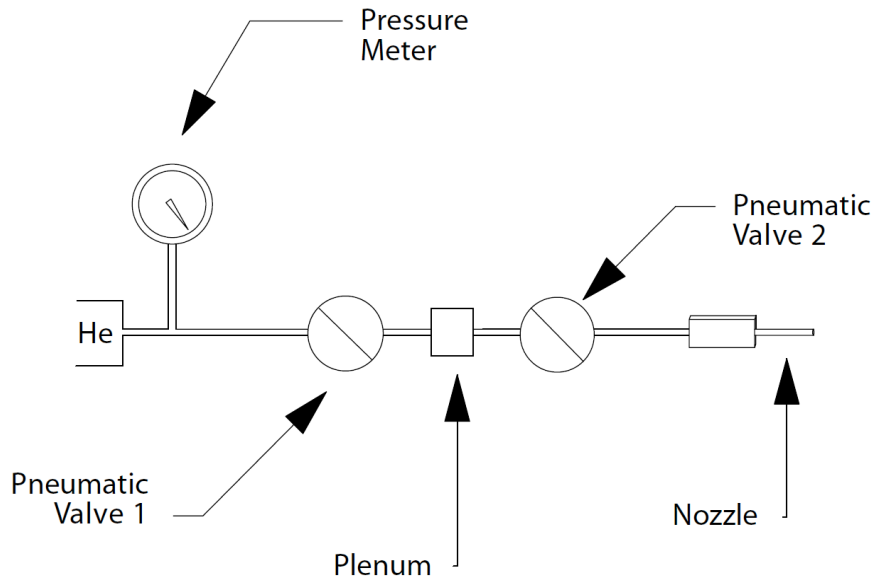

Fig. 2: Schematic of the gas puff system (not to scale).

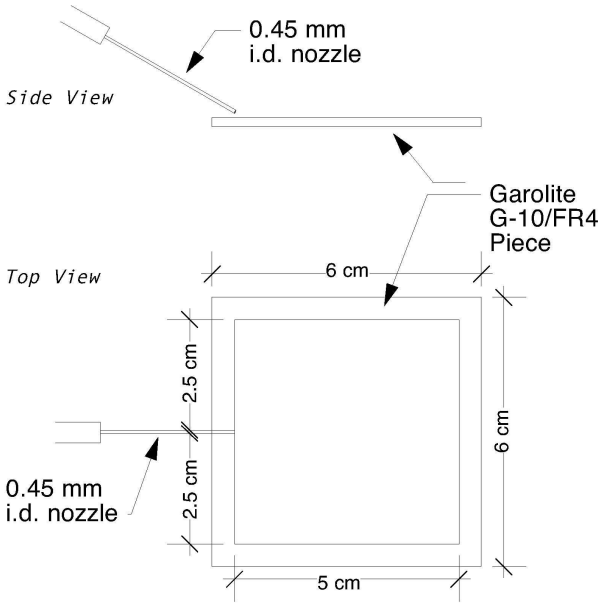

Fig. 3: Schematic of the setup used for tests to obtain the optimum plenum pressure and inclination angle of the puff system. The 6 cm x 6 cm area consists of the entire surface of the G-10 piece and the 5 cm x 5 cm area consists in the surface of the 51 mm detector to be cleared from residual dust.

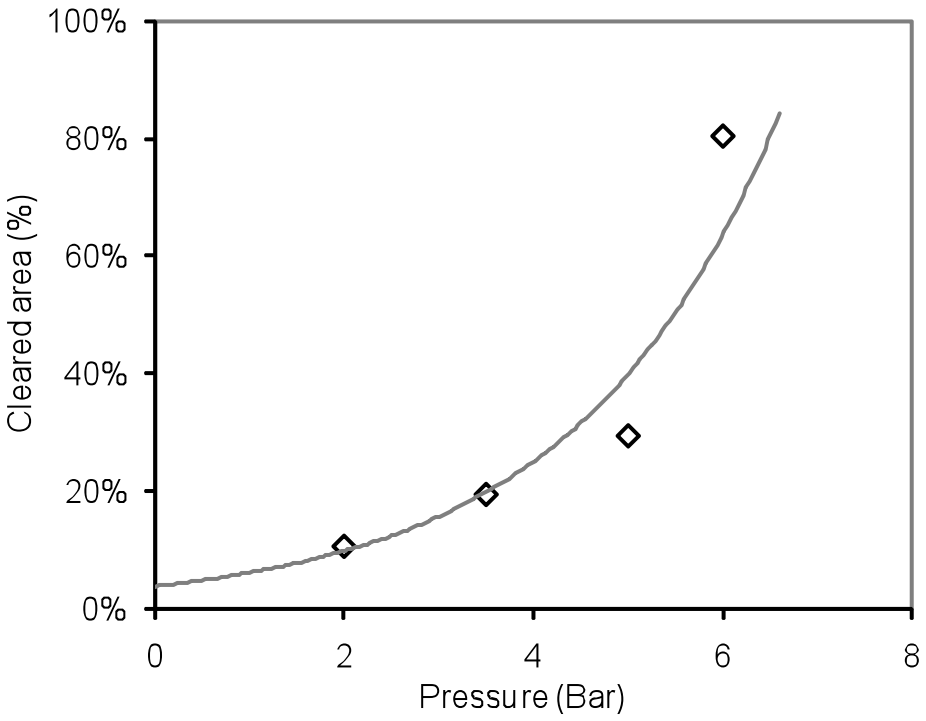

Fig. 4: Percentage of the cleared area vs. the backing He pressure with an incidence angle of 30º. One nozzle was aimed with 1 mm height from the detector. The experiment was conducted in air at atmospheric pressure.

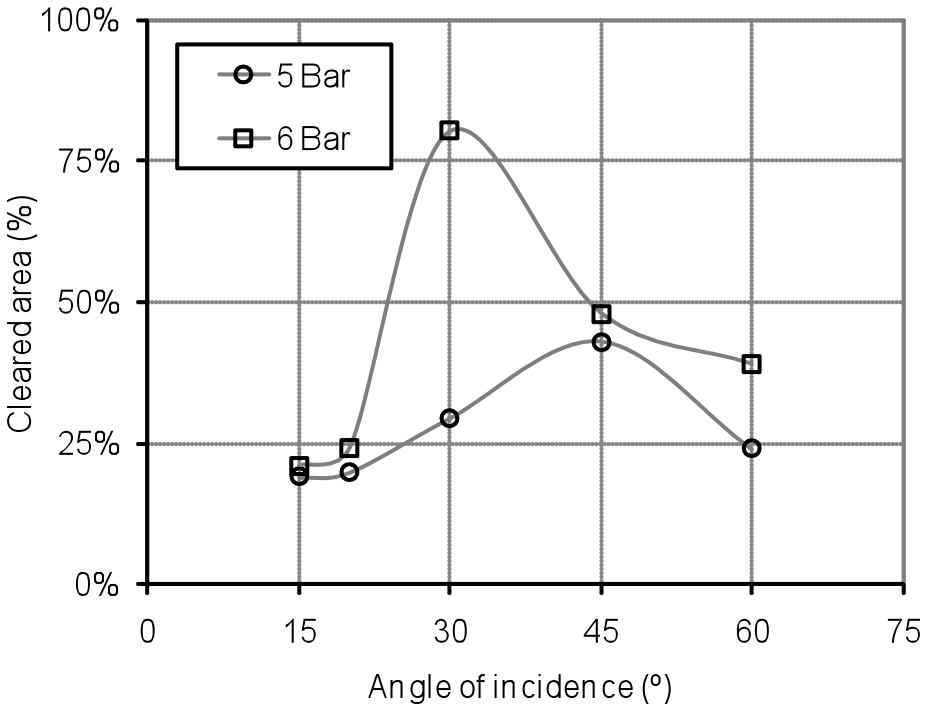

Fig. 5: The cleared area vs. the angle of incidence of the nozzle for 5 and 6 bar backing pressure. 1 mm distance separated the nozzle and the 5 cm x 5 cm area (surface of the electrostatic dust detector) and the experiment was conducted in air at atmospheric pressure. The cleared area % is defined as the area free of sand divided by the 5 cm x 5 cm area of the dust detector.

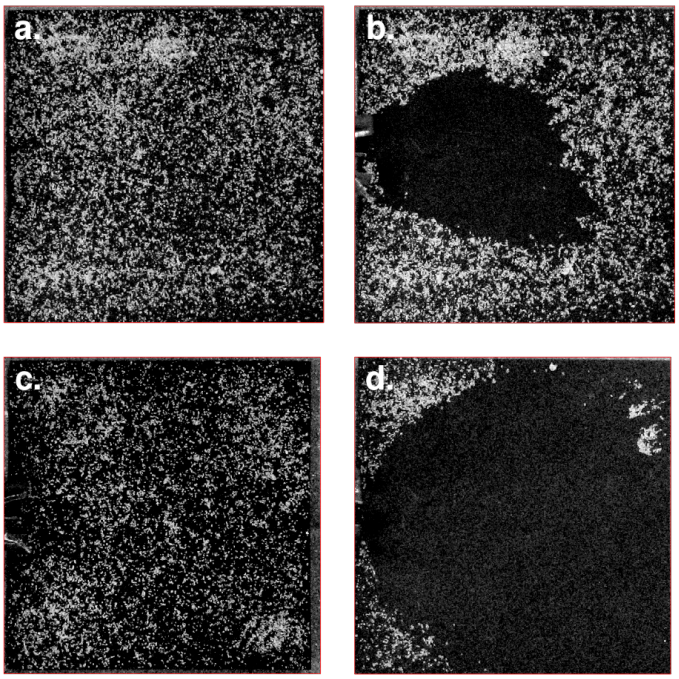

Fig. 6: Pictures of sand particles at atmospheric pressure taken with a digital camera before puff (a) and (c) and after puff (b) and (d) with one nozzle at 30º incidence. In image (b) the puff was performed with a plenum pressure of 5 bar and in image (d) with 6 bar. The puff was in the direction from left to right.

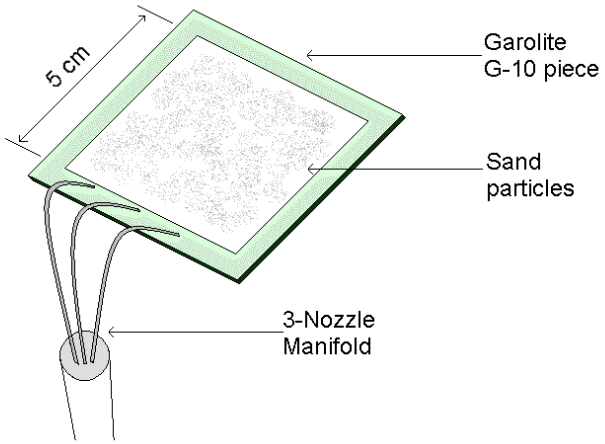

Fig. 7: Configuration of the three-nozzle puffer. The nozzles are aimed with a 30º incidence angle at 1mm above the 5 cm x 5 cm area (surface of the electrostatic dust detector). Sand particles were spread evenly of the 5 cm x 5 cm surface of the G-10 piece.

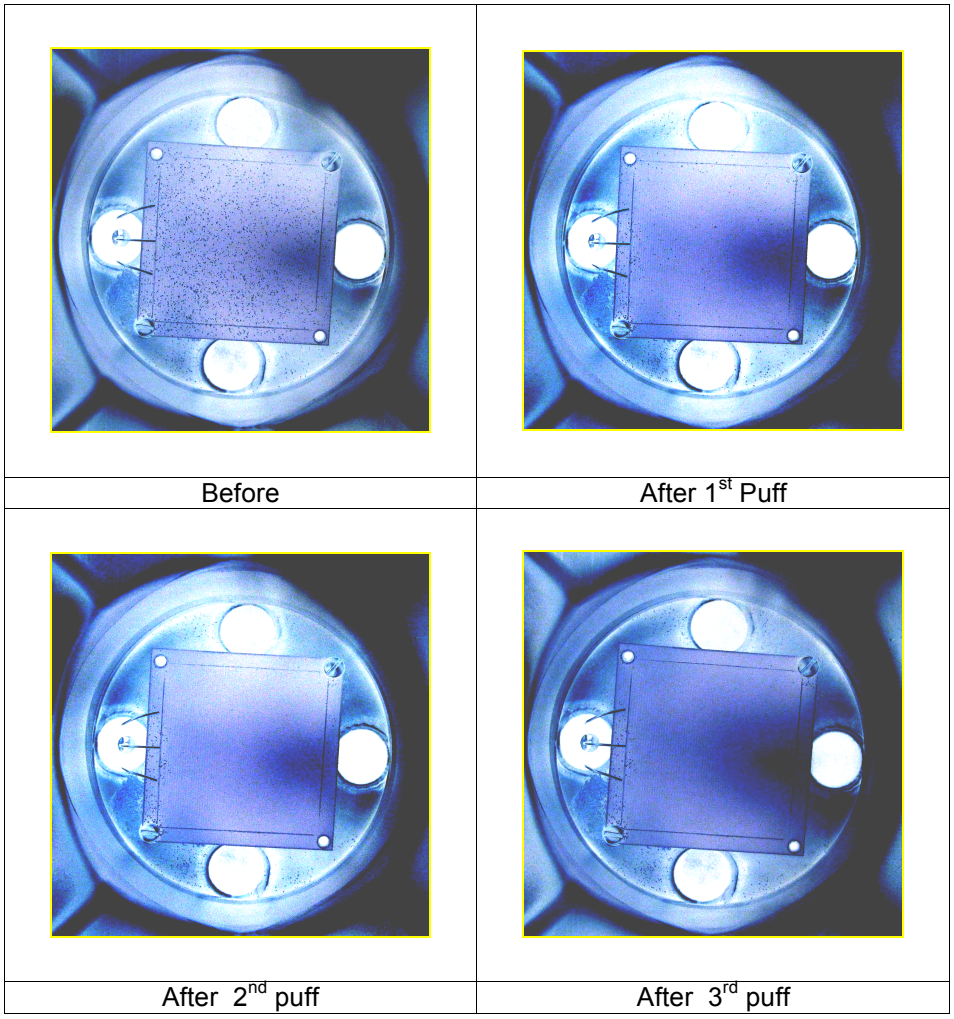

Fig. 8: Pictures of sand particles at atmospheric pressure taken with a digital camera before and after successive puffs. Puffing was achieved with the three-nozzle manifold with a 30º incidence angle and 6 bar plenum pressure. The three-nozzle manifold is localized on the left of the images and the puffs were achieved from left to right. The image has been color enhanced to make the sand particles more visible.

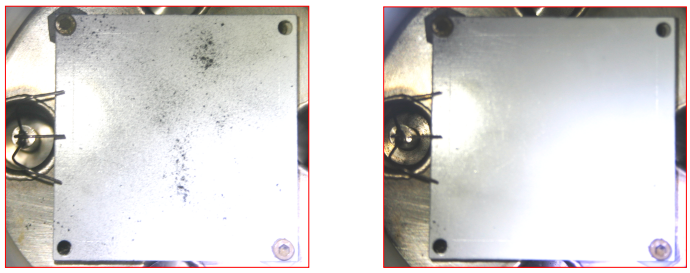

a. b.

Fig. 9: Pictures of carbon particles in air at atmospheric pressure taken with digital camera (a) before puff and (b) after puff. Puffing was performed with the three-nozzle manifold with a 30º incidence angle and 6 bar plenum pressure. The images did not undergo any color enhancement.

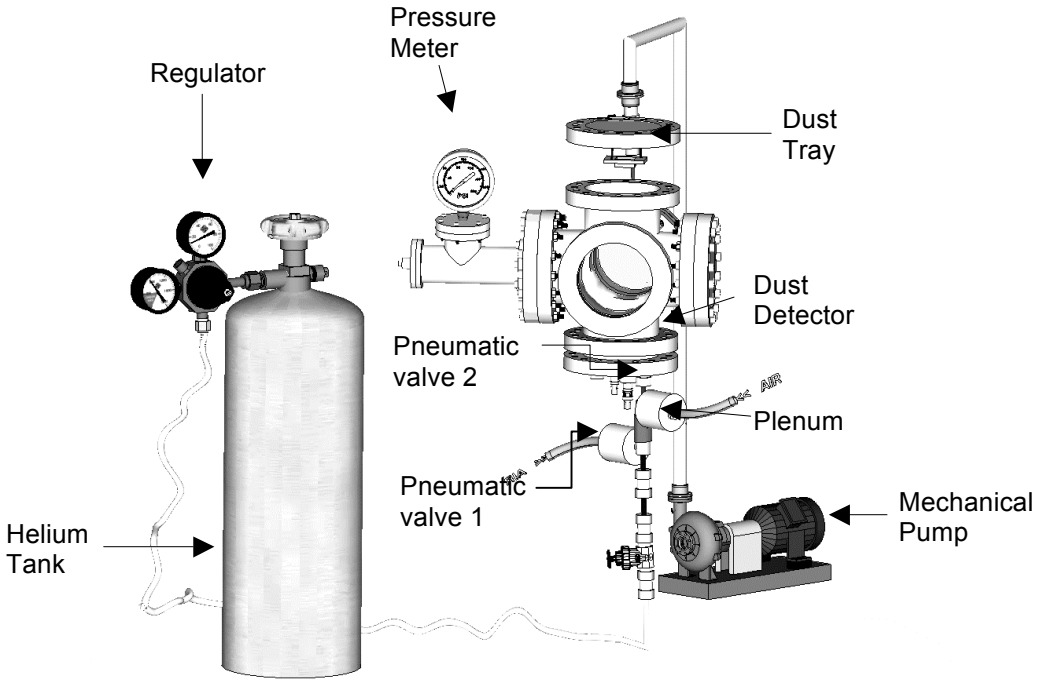

Fig. 10: Setup used for vacuum puffing.

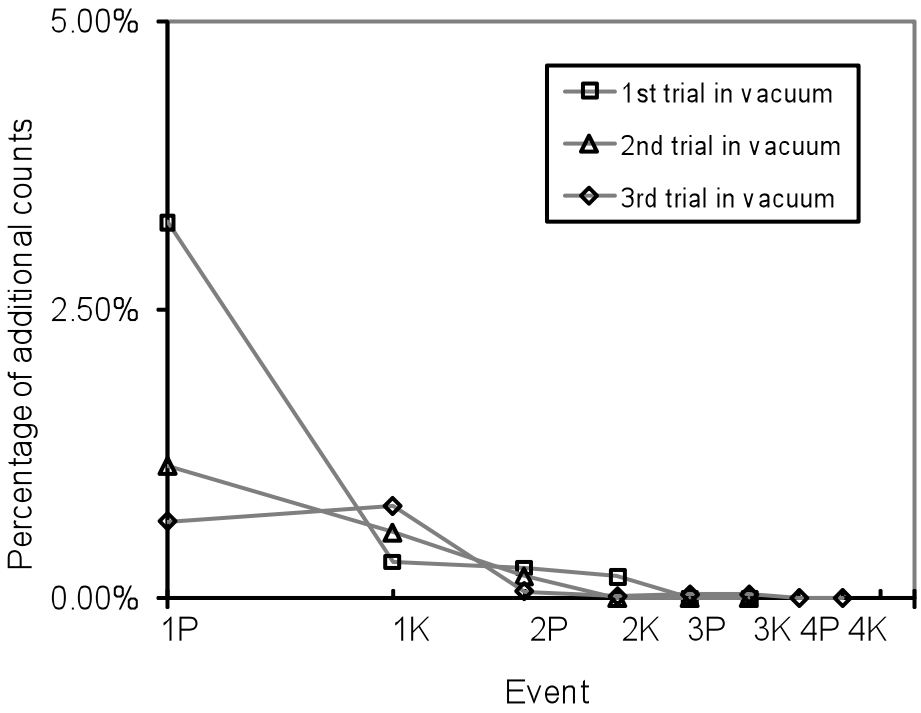

Fig. 11: Percentage of additional counts triggered by consecutive puffs labeled 1P, 2P, 3P … and knocks labeled 1K, 2K, 3K … in vacuum conditions without cover mesh and with the 3 nozzles manifold. For three trials the percentage of additional counts triggered by a knock event after a second puff was lower than 0.5%.

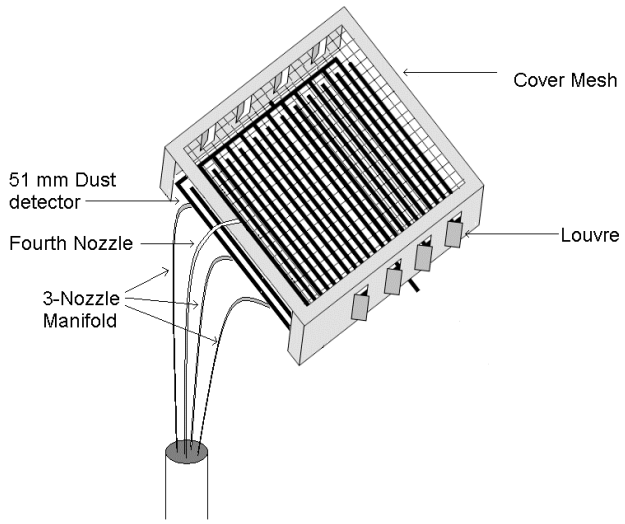

Fig. 12: Puff system setup with 51mm dust detector and cover mesh used in NSTX [4,5]. The detector is shown schematically by the thick lines under the cover mesh. For clarity the mesh porosity is not to scale. Three of the nozzles are aimed on the surface of the detector and the fourth nozzle is aimed on the surface of the mesh.

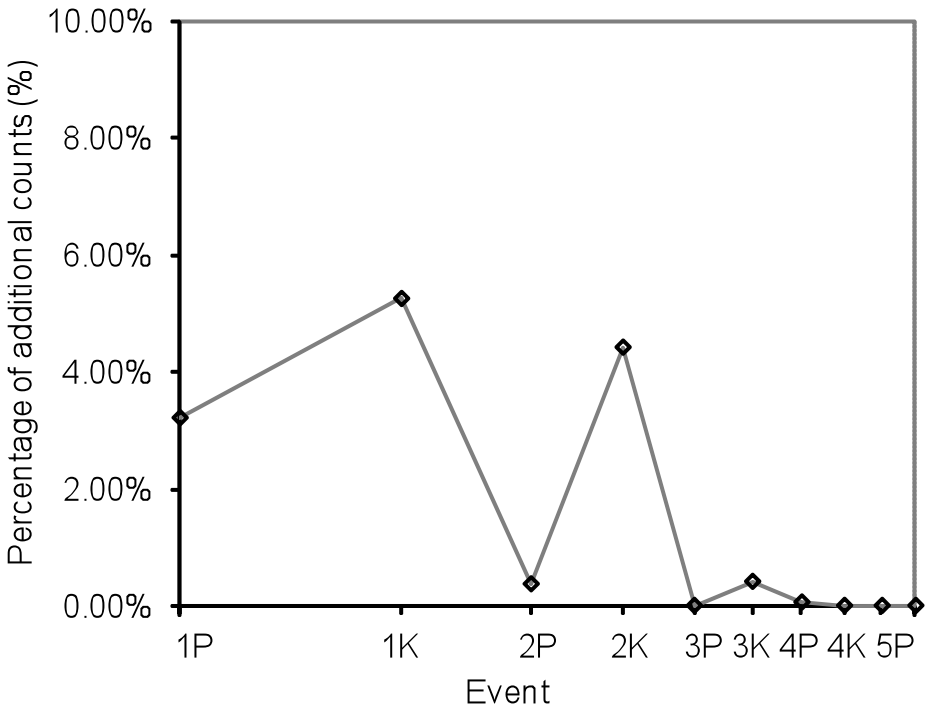

Fig. 13: Percentage of additional counts triggered by consecutive puffs labeled 1P, 2P, 3P … and knocks labeled 1K, 2K, 3K … in vacuum conditions with cover mesh and 4 nozzles manifold. After two puffs an insignificant number of additional counts were triggered by a knock event indicating that the entire surface of the detector was cleared.

References:

[1] G. Federici, C.H. Skinner, J.N. Brooks, J.P. Coad, C. Grisolia, A.A. Haasz, A. Hassanein, V. Philipps, C.S.Pitcher, J. Roth, W.R. Wampler, and D.G. Whyte, Nucl. Fus., 41, 1967 (2001).

[2] S. Rosanvallon, C. Grisolia, P. Andrew, S. Ciattaglia, P. Delaporte, D. Douai, D. Garnier, E. Gauthier, W. Gulden S.H. Hong, S. Pitcher, L. Rodriguez, N. Taylor, A. Tesini, S. Vartanian, A. Vatry, and M. Wykes, J. Nucl. Mater., 390-391 (2009) 57.

[3] ITER_Diagnostic_Project_Requirements_(PR)_27ZRW8_v4_0

[4] C.H. Skinner, B. Rais, A. L. Roquemore, H.W. Kugel, R. Marsala, T. Provost "First real-time detection of surface dust in a tokamak" PPPL report 4517 May 2010, Rev. Sci. Instrum. (2010) in press.

[5] B. Rais, C.H. Skinner, A.L. Roquemore "Absolute calibration of an electrostatic dust detector" PPPL report 4537 July 2010.

[6] C.V. Parker, C.H. Skinner and A.L. Roquemore, J. Nucl. Mater., 363- 365 (2007) 1461.

[7] A. Campos and C.H. Skinner, J. of Undergraduate Research IX (2009) 30. Available at http://www.scied.science.doe.gov/scied/JUR_v9/default.htm.

[8] G.F. Counsell, A.P.C. de Vere, N.St.J. Braithwaite, S. Hillier and P. Bjorkman, Rev. Sci. Instrum. 77 (2006), p. 093501.

[9] D.P. Boyle, C.H. Skinner, A.L. Roquemore, J. Nucl. Mater., 390-391 (2009) 1086

0041227187937

The Princeton Plasma Physics Laboratory is operated
by Princeton University under contract
with the U.S. Department of Energy.

Information Services
Princeton Plasma Physics Laboratory
P.O. Box 451
Princeton, NJ 08543

Phone: 609-243-2245
Fax: 609-243-2751
e-mail: pppl_info@pppl.gov
Internet Address: http://www.pppl.gov